View metadata, citation and similar papers at core.ac.uk
brought to you by CORE
provided by D-Scholarship@Pitt

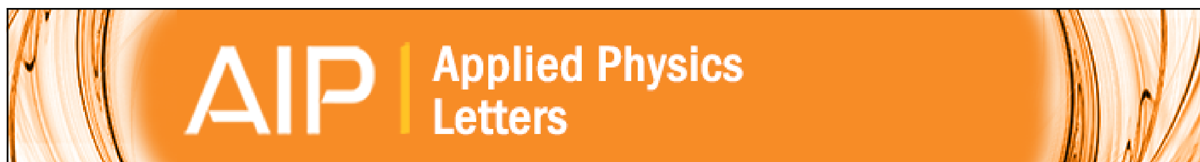

H-induced platelet and crack formation in hydrogenated epitaxial Si ∕ Si 0.98 B 0.02 ∕ Si structures

Lin Shao, Yuan Lin, J. G. Swadener, J. K. Lee, Q. X. Jia, Y. Q. Wang, M. Nastasi, Phillip E. Thompson, N. David Theodore, T. L. Alford, J. W. Mayer, Peng Chen, and S. S. Lau

Citation: Applied Physics Letters **88**, 021901 (2006); doi: 10.1063/1.2163992
View online: http://dx.doi.org/10.1063/1.2163992
View Table of Contents: http://scitation.aip.org/content/aip/journal/apl/88/2?ver=pdfcov
Published by the AIP Publishing

Articles you may be interested in
Sharp crack formation in low fluence hydrogen implanted Si0.75Ge0.25/B doped Si0.70Ge0.30/Si heterostructure
Appl. Phys. Lett. **103**, 142102 (2013); 10.1063/1.4823587

Cracking in hydrogen ion-implanted Si ∕ Si 0.8 Ge 0.2 ∕ Si heterostructures
Appl. Phys. Lett. **92**, 061904 (2008); 10.1063/1.2838338

Investigation of stress-induced (100) platelet formation and surface exfoliation in plasma hydrogenated Si
Appl. Phys. Lett. **91**, 244101 (2007); 10.1063/1.2822414

Integration of functional epitaxial oxides into silicon: From high- K application to nanostructures
J. Vac. Sci. Technol. B **25**, 1039 (2007); 10.1116/1.2720858

Relaxed graded SiGe donor substrates incorporating hydrogen-gettering and buried etch stop layers for strained silicon layer transfer applications
J. Appl. Phys. **101**, 013522 (2007); 10.1063/1.2405237

This article is copyrighted as indicated in the article. Reuse of AIP content is subject to the terms at: http://scitation.aip.org/termsconditions. Downloaded to IP: 130.49.166.8 On: Fri, 07 Nov 2014 19:52:16

H-induced platelet and crack formation in hydrogenated epitaxial $Si/Si_{0.98}B_{0.02}/Si$ structures

Lin Shao,[a] Yuan Lin, J. G. Swadener, J. K. Lee, Q. X. Jia, Y. Q. Wang, and M. Nastasi
Los Alamos National Laboratory, Los Alamos, New Mexico 87545

Phillip E. Thompson
Code 6812, Naval Research Laboratory, Washington, DC 20375-5347

N. David Theodore
Advanced Products Research and Development Laboratory, Freescale Semiconductor Inc., Tempe, Arizona 85284

T. L. Alford and J. W. Mayer
Department of Chemical and Materials Engineering, Arizona State University, Tempe, Arizona 85287

Peng Chen and S. S. Lau
University of California at San Diego, La Jolla, California 92093

(Received 26 August 2005; accepted 9 December 2005; published online 9 January 2006)

An approach to transfer a high-quality Si layer for the fabrication of silicon-on-insulator wafers has been proposed based on the investigation of platelet and crack formation in hydrogenated epitaxial $Si/Si_{0.98}B_{0.02}/Si$ structures grown by molecular-beam epitaxy. H-related defect formation during hydrogenation was found to be very sensitive to the thickness of the buried $Si_{0.98}B_{0.02}$ layer. For hydrogenated Si containing a 130 nm thick $Si_{0.98}B_{0.02}$ layer, no platelets or cracking were observed in the B-doped region. Upon reducing the thickness of the buried $Si_{0.98}B_{0.02}$ layer to 3 nm, localized continuous cracking was observed along the interface between the Si and the B-doped layers. In the latter case, the strains at the interface are believed to facilitate the (100)-oriented platelet formation and (100)-oriented crack propagation. © *2006 American Institute of Physics*.
[DOI: 10.1063/1.2163992]

Recently, there has been extensive interest in the phenomenon of hydrogen-induced exfoliation of silicon.[1,2] Various studies have contributed to a commercialized "ion-cut" process for the fabrication of silicon-on-insulator (SOI) wafers, which provides substrates needed for fabrication of advanced Si devices.[1,2] In the conventional ion-cut technique (Smart-cut™) hydrogen is introduced by ion implantation and the thickness of the transferred layer is controlled by adjusting the energy of the implanted H ions.[1] H implantation and subsequent annealing create hydrogen-terminated cavities near the damage peak.[2] These cavities evolve into cracks running parallel to the surface that finally allow the surface layer to be separated from the substrate.[3,4] To meet the demands of next-generation device fabrication, future SOI wafers will require the top Si layers to be less than 100 nm thick.[5] However, simply reducing the hydrogen ion energy is insufficient to realize the transfer of ultrathin layers.[6] In several improvements of ion-cut techniques, heavy ion implantation (e.g., Si or Ar) or dopant implantation (e.g., B) is used to form a H trapping layer.[7,8] These methods, however, have the disadvantage of degrading the crystalline quality of the transferred layers due to ion-irradiation-induced damage.

In an attempt to overcome some of the limitations associated with ion implantation derived ion-cut, we have studied B-doping effects on hydrogenation-induced crack formation in Si with B atoms incorporated by epitaxial growth. This work was motivated by the need to develop a new method for the transfer of ultrathin Si layers with significant improvements in crystalline quality and smoothness of the transferred layers.

Samples used in this study were grown by molecular-beam epitaxy (MBE). In one epitaxial $Si/Si_{0.98}B_{0.02}/Si$ sample, the $Si_{0.98}B_{0.02}$ layer was 3 nm thick and was deposited at a depth of 200 nm beneath the surface. In another $Si/Si_{0.98}B_{0.02}/Si$ sample, the $Si_{0.98}B_{0.02}$ layer was 130 nm thick and was deposited in a depth region of 100 to 230 nm beneath the surface. Both samples were hydrogenated for 3 h, in an inductively coupled plasma (ICP) system with an ICP power of 100 W and a reactive ion etching power of 500 W. Before hydrogenation, the sample surfaces were treated with an oxygen plasma. For purposes of comparison, a virgin Si control sample without B doping was hydrogenated simultaneously. All samples used in this study were (100) oriented.

Depth distributions of hydrogen were measured using elastic recoil detection (ERD) analysis. ERD analysis was performed using a 3.0 MeV $^4He^+$ beam oriented 75.3° from the sample normal. The detector was positioned 150.5° away from the incident beam. A 14 μm thick Mylar® foil was placed between the sample and the detector. Transmission electron microscopy (TEM) was used to characterize the samples before and after hydrogenation. Optical microscopy with Nomarski lenses was used to detect bubble formation on the sample surface after hydrogenation. High-resolution x-ray diffraction (XRD) analyses were used to measure strains in the samples. An ω-2θ scan around Si (004) was collected using a Bede D1 x-ray diffractometer. Strain depth profiles are obtained from Bede RADS auto-fit to the corresponding XRD data.

[a]Electronic mail: lshao@mailaps.org

This article is copyrighted as indicated in the article. Reuse of AIP content is subject to the terms at: http://scitation.aip.org/termsconditions. Downloaded to IP: 130.49.166.8 On: Fri, 07 Nov 2014 19:52:16

 © 2006 American Institute of Physics

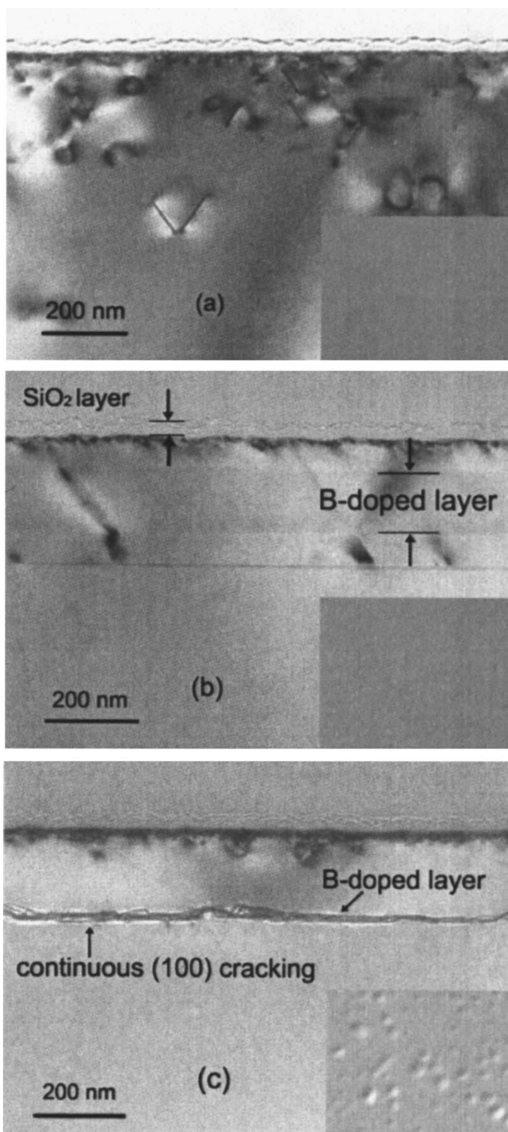

FIG. 1. TEM micrographs from hydrogenated virgin Si (a), hydrogenated MBE Si containing a 130 nm thick $Si_{0.98}B_{0.02}$ layer (b), and hydrogenated MBE Si containing a 3 nm thick $Si_{0.98}B_{0.02}$ layer (c). The insets are optical images of the sample surfaces.

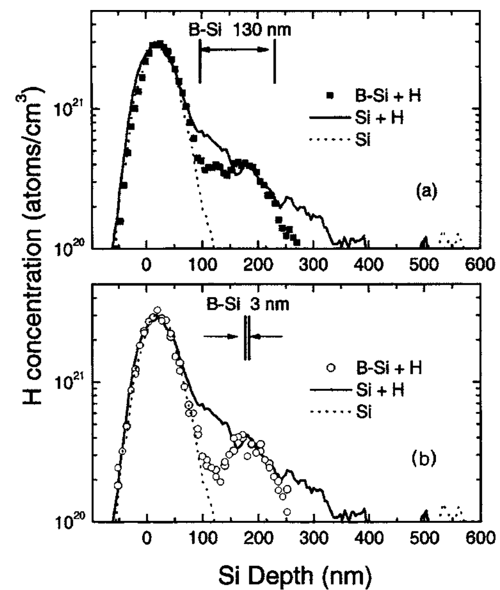

FIG. 2. ERD spectra showing H concentration vs depth for hydrogenated MBE Si (B-Si+H) containing a 130 nm thick $Si_{0.98}B_{0.02}$ layer (a) and for hydrogenated MBE Si containing a 3 nm thick $Si_{0.98}B_{0.02}$ layer (b). H distributions within the control Si (without B doping) before (Si) and after hydrogenation (Si+H) are also plotted for comparison.

The cross-sectional TEM micrograph presented in Fig. 1(a) shows platelet formation in the hydrogenated virgin Si (without B doping). A dense band of (111) oriented platelets is observed over a depth range of 0 to 300 nm and a few platelets are also observed at depths of up to 600 nm. No cracking is observed. The inset within Fig. 1(a) is an optical image of the hydrogenated sample surface; no surface blistering is present.

Figure 1(b) presents a cross-sectional TEM micrograph obtained from the hydrogenated Si containing a 130 nm thick $Si_{0.98}B_{0.02}$ layer buried 100 nm beneath the surface. No cracking and no platelets are observed and the optical image inset shows no obvious signs of bubbles. The few defects observed in Fig. 1(b) are threading dislocations and microtwins, which originate from the interface and propagate to the surface. These defects are formed during MBE growth since the same type of defects are observed in the same sample before hydrogenation (not shown).

A striking difference is seen upon reducing the thickness of the buried epitaxial $Si_{0.98}B_{0.02}$ layer to 3 nm. Figure 1(c) shows a TEM micrograph obtained from the hydrogenated Si containing a 3 nm thick $Si_{0.98}B_{0.02}$ layer. At the depth of the B-doped layer, there is a continuous (100) oriented crack that has formed. Intense surface bubbling is observed by optical microscopy, as revealed in the inset. Furthermore, when compared with the TEM micrograph of the hydrogenated virgin Si [Fig. 1(a)], Figure 1(c) shows that (111) platelet formation is significantly suppressed in the top Si layer, the portion to be transferred to form SOI wafers.

All three TEM micrographs in Fig. 1 show the formation of a silicon oxide layer around 30 nm thick on the surface, which is due to the oxygen plasma treatment prior to hydrogenation. The oxide layer was confirmed by Rutherford backscattering spectrometry to be $SiO_{1.8\pm0.1}$ with a thickness of 34 nm. The intent of the surface oxide layer is to reduce surface contamination and to reduce defect creation near the surface region during hydrogenation.

ERD measurements from the hydrogenated samples show that H profiles are virtually coincident with the B dopant profile. Figure 2(a) shows that the H distribution has a boxlike shape in the 130 nm thick B-doped region. Figure 2(b) shows a H trapping peak at the depth of the 3 nm thick B-doped layer. The peak H concentration is around $4\times10^{20}/cm^3$ within the doping region for both the thick and thin B-doped layers. For the hydrogenated control sample, H is observed for depths up to 400 nm [given as solid lines in Figs. 2(a) and 2(b)], with the concentration reaching a value of around $2\times10^{20}/cm^3$ at 300 nm, the depth where (111) platelet formation terminates [Fig. 1(a)].

The observations of (111)-oriented platelets in the intrinsic Si [Fig. 1(a)] and the absence of platelets in the MBE-grown samples [Figs. 1(b) and 1(c)] can be explained by the presence of B in top MBE-grown Si layers and the platelet formation model proposed by Nickel *et al.*[9] Secondary ion mass spectrometry measurements revealed both top Si layers are slightly doped with B at a density of around $3\times10^{17}/cm^3$ and Nickel's work shows that (111) platelet

This article is copyrighted as indicated in the article. Reuse of AIP content is subject to the terms at: http://scitation.aip.org/termsconditions. Downloaded to IP: 130.49.166.8 On: Fri, 07 Nov 2014 19:52:16

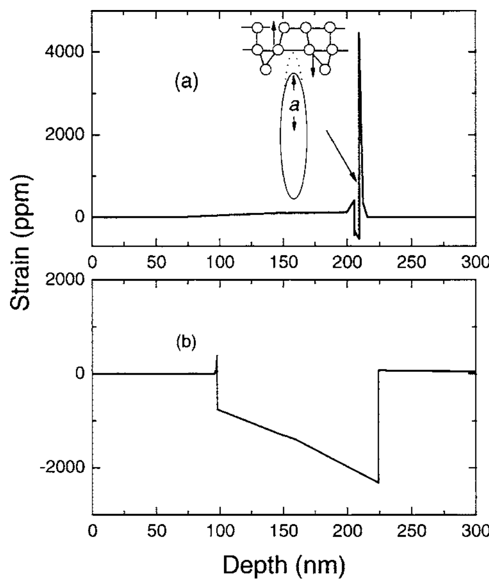

FIG. 3. Out-of-plane strains as a function of depth for hydrogenated MBE Si containing a 3 nm thick $Si_{0.98}B_{0.02}$ layer (a) and hydrogenated MBE Si containing a 130 nm thick $Si_{0.98}B_{0.02}$ layer (b). In (a), a schematic illustration of a crack propagating under the influence of strains is included.

formation during hydrogenation is favored in *n*-type Si, but not favored in *p*-type Si.[9]

The continuous cracking formed at the depth of the 3 nm B-doped layer [Fig. 1(c)] has a (100) orientation and therefore the cracking is not dependent on (111) platelet formation. We believe that strain plays an important role in this phenomena. Figure 3(a) shows the strain-depth profile, deduced from the XRD analysis, in the as-grown Si containing a 3 nm thick B-doped layer. An out-of-plane tensile strain exists in the Si, at the interface, on both sides of the B-doped layer. The B-doped layer possesses an out-of-plane compressive strain. Due to Poisson's effect,[10] the strains at the interface correspond an in-plane compressive strain in the Si layer and an in-plane tensile strain in the B-doped layer, which places the interface in a state of shear. Based on our previous studies on platelet and crack formation in hydrogen-ion-implanted Si and hydrogenated Si containing a buried SiGe layer,[4,11] we believe that strain facilitates the (100)-oriented cracking through three successive steps:

(1) Vacancies are kinetically and thermodynamically predisposed to agglomerate in regions of in-plane compressive strain. High-resolution electron microscopy of electron-irradiated compressively strained SiGe has shown preferential aggregation of vacancies on (100) planes.[12] Vacancy generation can occur during MBE growth and surface ion bombardment of the hydrogenation process.

(2) Formation of (100)-oriented platelets is facilitated due to the interaction of H with vacancy agglomerates. Various studies have proposed that vacancies play a central role in platelet formation.[3,4,13]

(3) Cracking along (100) plane is facilitated due to the presence of an interface shear strain. Once (100)-oriented platelets are formed, the shear strain can facilitate cracking along the interface. The kinetics of cracking can be described by[14]

$$J = \frac{P^2 + \tau^2}{E}(1 - \nu^2)\frac{4}{\pi}a, \tag{1}$$

where J is energy release rate (or driving force for crack propagation), E is Young's modulus, ν is Poisson's ratio, P is the pressure inside the platelet, τ is the shear stress, and a is the radius of the platelet. As shown schematically in the inset in Fig. 3(a), the sheer strains help to break the Si bonds for crack propagation. The fracture occurs only when J is above a threshold value, or equivalently, when platelets reach a threshold radius a_C. Due to the contribution of shear strains, cracking could occur for small platelets with their radius a being less than a_C of normal cracking cases (without shear strains). This provides a possible explanation for why continuous cracking is present along the interface in Fig. 1(c). As for the Si containing a 130 nm thick B-doped layer, the strain depth profile [Fig. 3(b)] shows a strain that decreases with decreasing depths. A very small shear strain at the shallow interface and an even smaller shear strain at the deep interface [the tensile strain in Si is hardly visible in Fig. 3(b)] are observed. Therefore, the strain distribution in the thick B-doped layer will not significantly facilitate (100) cracking.

Our studies show that the epitaxial $Si/Si_xB_{1-x}/Si$ structure can be used to transfer a high-quality ultrathin Si layer if the B-doped layer is only a few nanometer thick. The cracking location can be controlled by the depth of the B-doped layer. The top Si layer sustains good crystalline quality after hydrogenation.

This research is supported by the Department of Energy, Office of Basic Energy Science, and by the Office of Naval Research. Two of the authors (U.C.S.D. and A.S.U.) gratefully acknowledge sponsorship from National Science Foundation (DMR-0308127, L. Hess).

[1]M. Bruel, Nucl. Instrum. Methods Phys. Res. B **108**, 313 (1996).
[2]T. Höchbauer, A. Misra, M. Nastasi, and J. W. Mayer, J. Appl. Phys. **89**, 5980 (2001).
[3]M. K. Weldon, V. E. Marsico, Y. J. Chabal, A. Agarwal, D. J. Eaglesham, J. Sapjeta, W. L. Brown, D. C. Jacobson, Y. Caudano, S. B. Christman, and E. E. Chaban, J. Vac. Sci. Technol. B **15**, 1065 (1997).
[4]M. Nastasi, T. Höchbauer, J. K. Lee, A. Misra, J. P. Hirth, M. Ridgway, and T. Lafford, Appl. Phys. Lett. **86**, 154102 (2005).
[5]*International Technology Roadmap for Semiconductors* (Semiconductor Industry Association, Palo Alto, CA, 2003), http://public.itrs.net
[6]C. Qian, B. Terreault, and S. C. Gujrathi, Nucl. Instrum. Methods Phys. Res. B **175–177**, 711 (2001).
[7]A. Usenko, J. Electron. Mater. **32**, 872 (2003).
[8]P. Chen, P. K. Chu, T. Höchbauer, J.-K. Lee, M. Nastasi, D. Buca, S. Mantl, R. Loo, M. Caymax, T. Alford, J. W. Mayer, N. D. Theodore, M. Cai, B. Schmidt, and S. S. Lau, Appl. Phys. Lett. **86**, 031904 (2005).
[9]N. H. Nickel, G. B. Anderson, N. M. Johnson, and J. Walker, Phys. Rev. B **62**, 8012 (2000).
[10]G. Dieter, *Mechanical Metallurgy*, 3rd ed. (McGraw-Hill, New York, 1986).
[11]L. Shao, Y. Lin, J. K. Lee, Q. X. Jia, Y. Q. Wang, M. Nastasi, P. E. Thompson, N. David Theodore, P. K. Chu, T. L. Alford, J. W. Mayer, P. Chen, and S. S. Lau, Appl. Phys. Lett. **87**, 091902 (2005).
[12]L. Fedina, O. I. Lebedev, G. Van Tendeloo, J. Van Landuyt, O. A. Mironov, and E. H. C. Parker, Phys. Rev. B **61**, 10336 (2000).
[13]F. A. Reboredo, M. Ferconi, and S. T. Pantelides, Phys. Rev. Lett. **82**, 4870 (1999).
[14]H. Tada, P. C. Paris, and G. R. Irwin, *The Stress Analysis of Cracks Handbook* (Del Research Corp., Hellertown, PA, 1985).

This article is copyrighted as indicated in the article. Reuse of AIP content is subject to the terms at: http://scitation.aip.org/termsconditions. Downloaded to IP: 130.49.166.8 On: Fri, 07 Nov 2014 19:52:16